

Supplementary Information

**Self-powered seesaw structured spherical buoys based on hybrid triboelectric-electromagnetic nanogenerator for sea surface wireless positioning**

Hongxin Hong, ‡<sup>a</sup> Xiya Yang, ‡<sup>a,\*</sup> Hui Cui,<sup>a,b</sup> Duo Zheng,<sup>a</sup> Haiyang Wen,<sup>a</sup> Ruiyuan Huang,<sup>a</sup>

Liqiang Liu,<sup>c</sup> Jialong Duan,<sup>a</sup> Qunwei Tang<sup>a,\*</sup>

<sup>a</sup> Institute of New Energy Technology, College of Information Science and Technology, Jinan University, Guangzhou 510632, PR China;

<sup>b</sup> College of Mechanical and Electronic Engineering, Shandong University of Science and Technology, Qingdao 266510, PR China;

<sup>c</sup> School of Electronics and Information Engineering, Tongji University, Shanghai 201804, PR China.

E-mail: xiyayang@jnu.edu.cn; tangqunwei@jnu.edu.cn

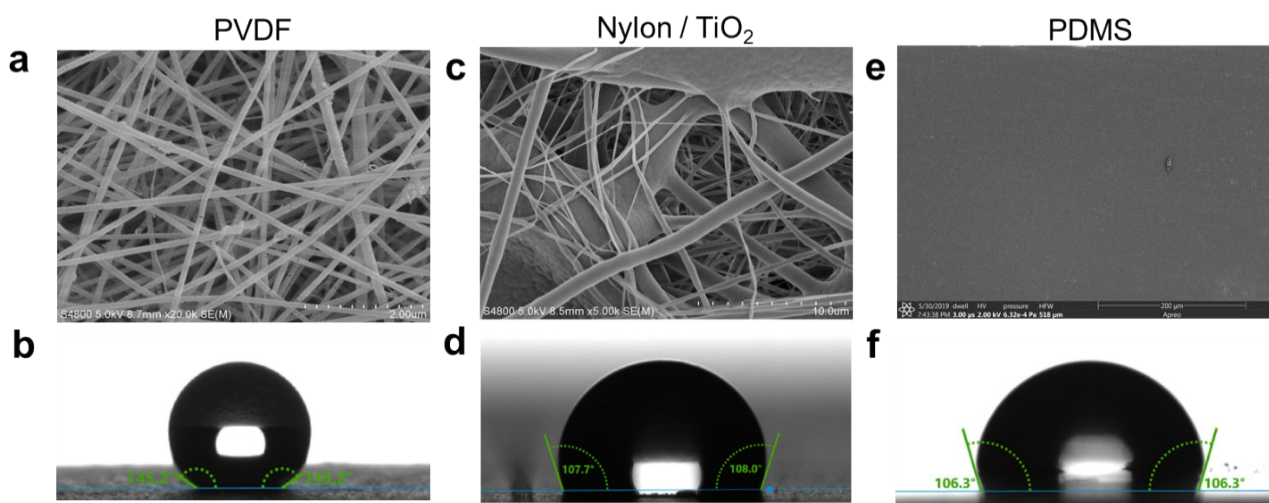


**Figure S1.** SEM morphology and water contact angle characterizations of (a, b) Electrospun PVDF, (c, d) Nylon/TiO<sub>2</sub> and (e, f) PDMS films.

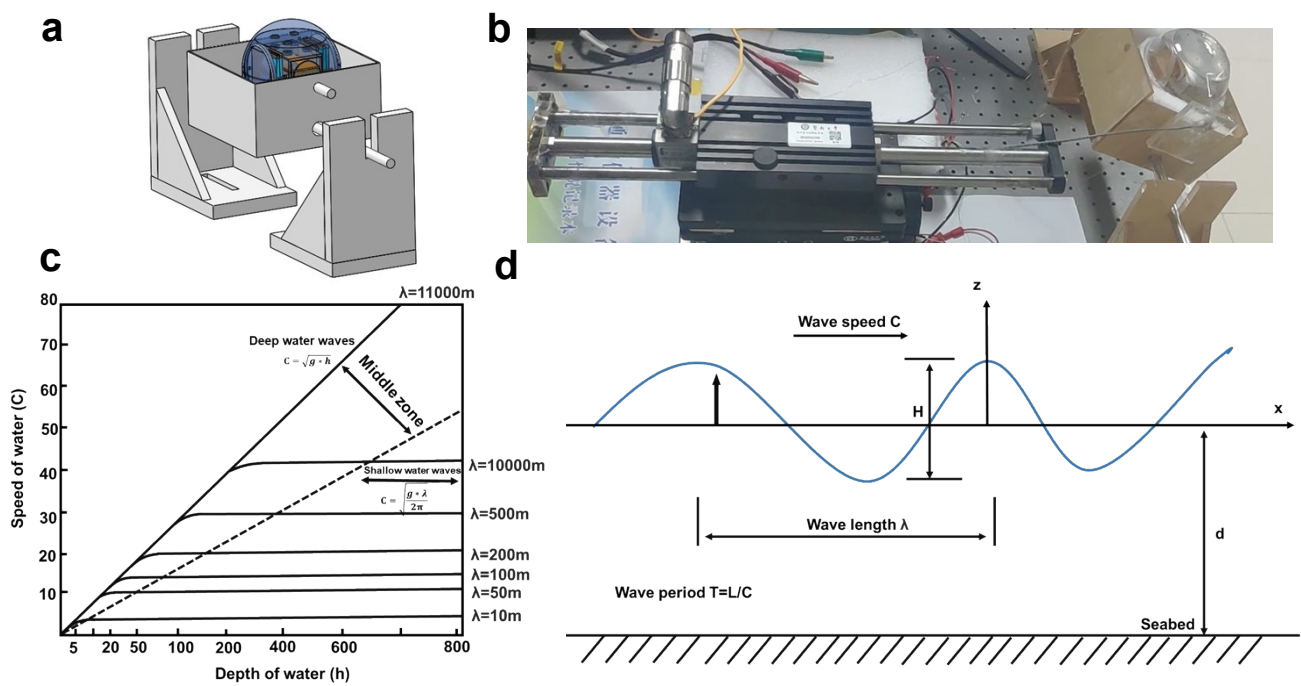


**Figure S2.** Setup for the measurement of the SSTE-HNG by fixing it in an acrylic box and drive by the linear motor to simulate the ocean waves.

To investigate the impact of the laminated layers on the power output and charge generation for the OZ-module, the layer number ranging from one to five were selected to study the effect. Theoretically, the more layers of the origami structure, the larger effective contact area for generating the triboelectrification charges and the higher power output. The transferred charges ( $Q_{sc}$ ) behaved an increasing trend as the origami layers increased from one to four layers, and a champion output was achieved at four layers. However, the transferred charges decreased rapidly when the origami layers further increased to five, which is mainly attributed to the limited contact-separation distance ( $d$ ) of the OZ module.

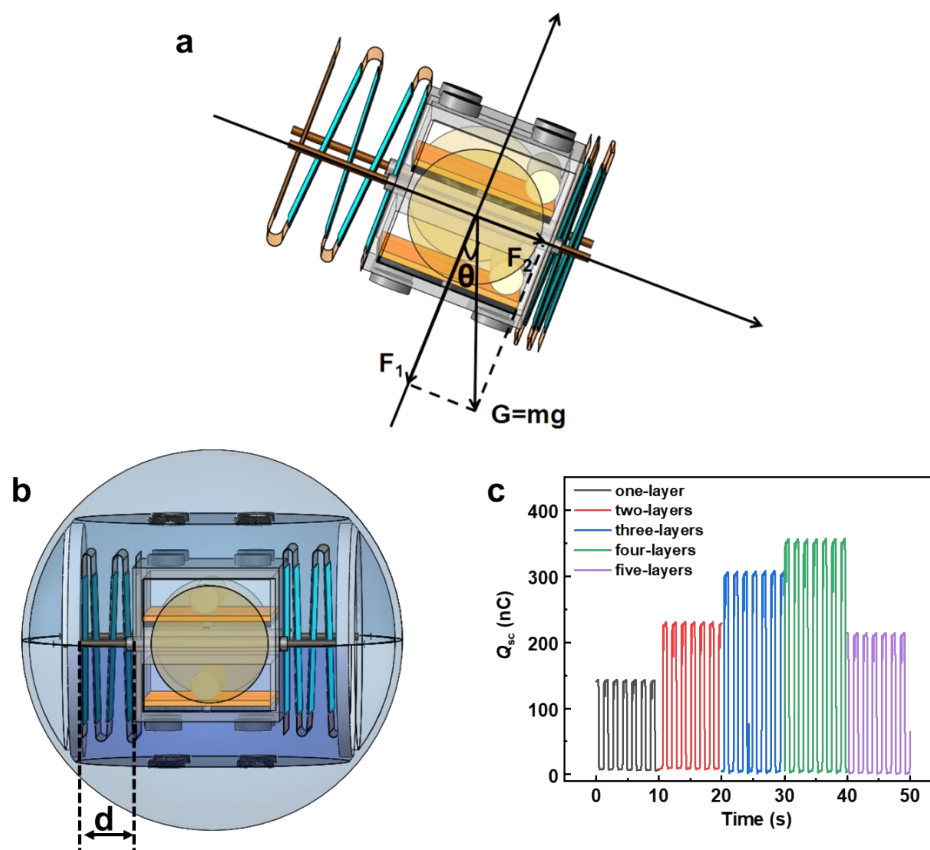


**Figure S3.** (a) Force analysis diagram when the OZ module is stretched and squeezed by the central slider. (b, c) Impact of the laminated layers on the power output and charge generation for the OZ module.

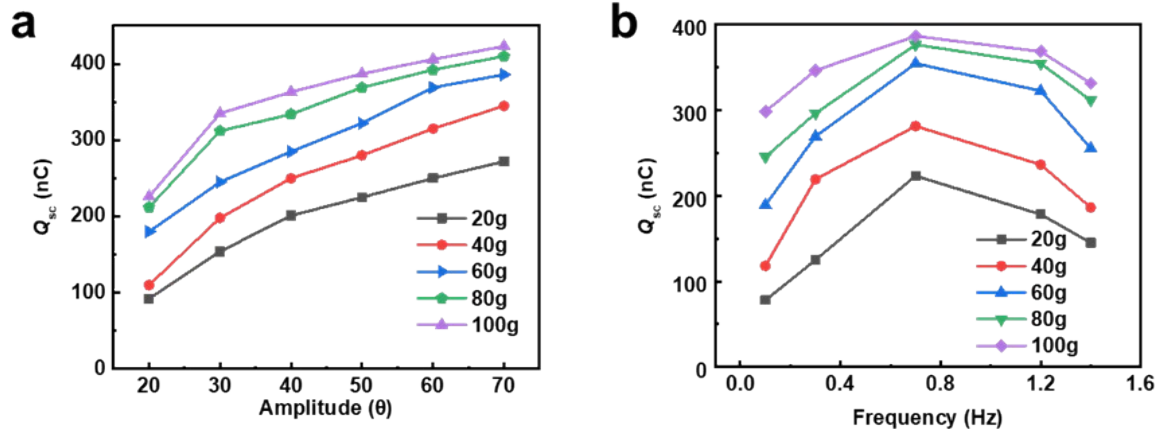


**Figure S4.** (a) The impact of the slider weight ranging from 20 to 100g on the output performance of SSTE-HNG under swing amplitudes from 20° to 70°. (b) The impact of the change of slider quality from 20 to 100g on the output performance of SSTE-HNG under frequencies from 0.1 to 1.4Hz.

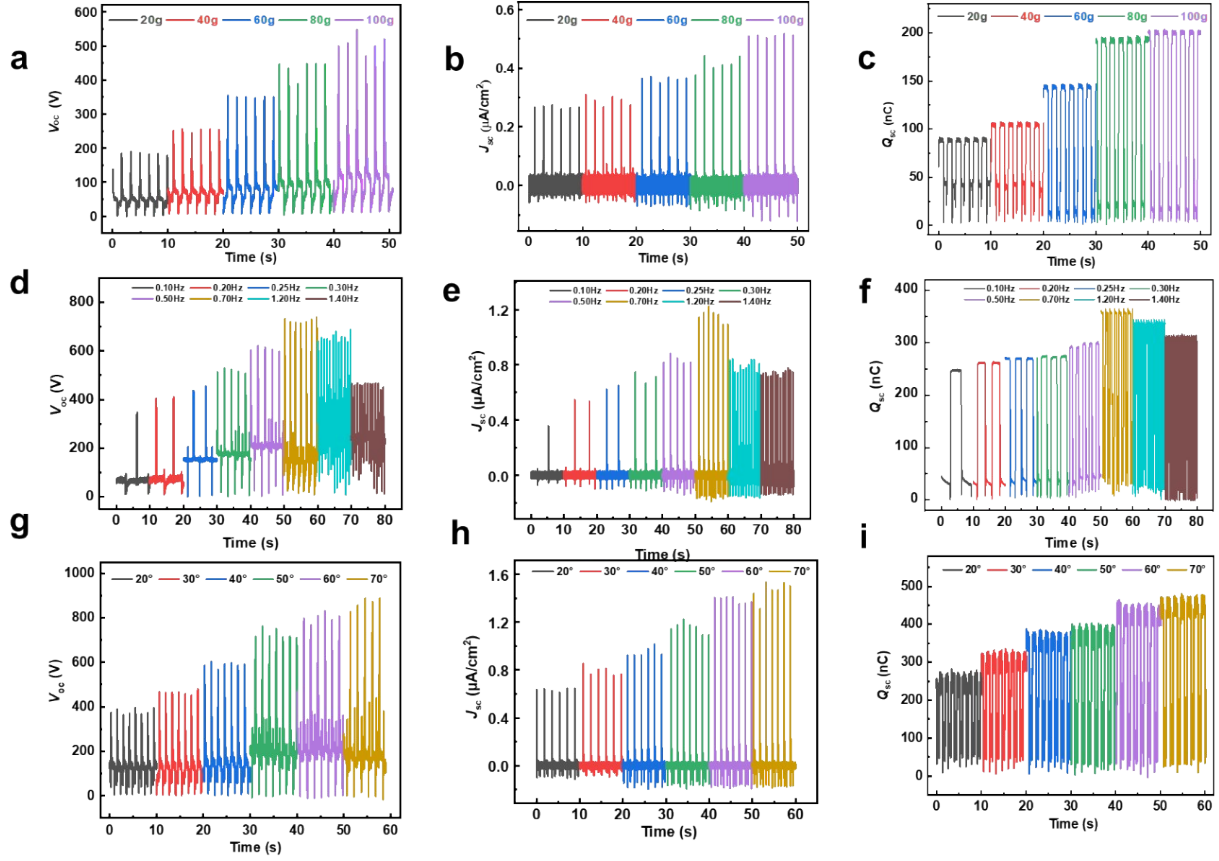


**Figure S5.** (a-c)  $V_{oc}$ ,  $J_{sc}$  and  $Q_{sc}$  of the OZ-module at various masses of Brass block. the swing angle  $\theta$  and the water wave frequency were fixed at  $20^\circ$  and 0.7 Hz respectively. (d-e)  $V_{oc}$ ,  $J_{sc}$  and  $Q_{sc}$  of STE-HNG at different frequency of function generator. The copper block mass and the swing angle  $\theta$  were fixed at 60g and  $50^\circ$  respectively. (g-f)  $V_{oc}$ ,  $J_{sc}$  and  $Q_{sc}$  of SSTE-HNG at different swing angle  $\theta$  of function generator. The copper block mass and the frequency were fixed at 60g and 0.7Hz respectively.

The magnetic induction field strength is measured by a Tesla meter with a magnitude of around 0.2T, which is comparable to the simulated value by COMSOL. Regarding the calculation of the induced electromotive force (*emf.*), which can be calculated from the given equation:

$$emf. = - N \times \Delta\phi / \Delta t \quad \text{Equation S1}$$

Where N is the number of turns of the induction coil, and  $\Delta\phi / \Delta t$  is the rate of change of magnetic flux. Substitute the values into the equation (N=500, B = 0.2T,  $\Delta t=0.03s$ ), the *emf.* is calculated to be 0.26V, which is close to the measured voltage output.

**a**



**Figure S6.** The magnetic induction field strength is measured by a Tesla meter.

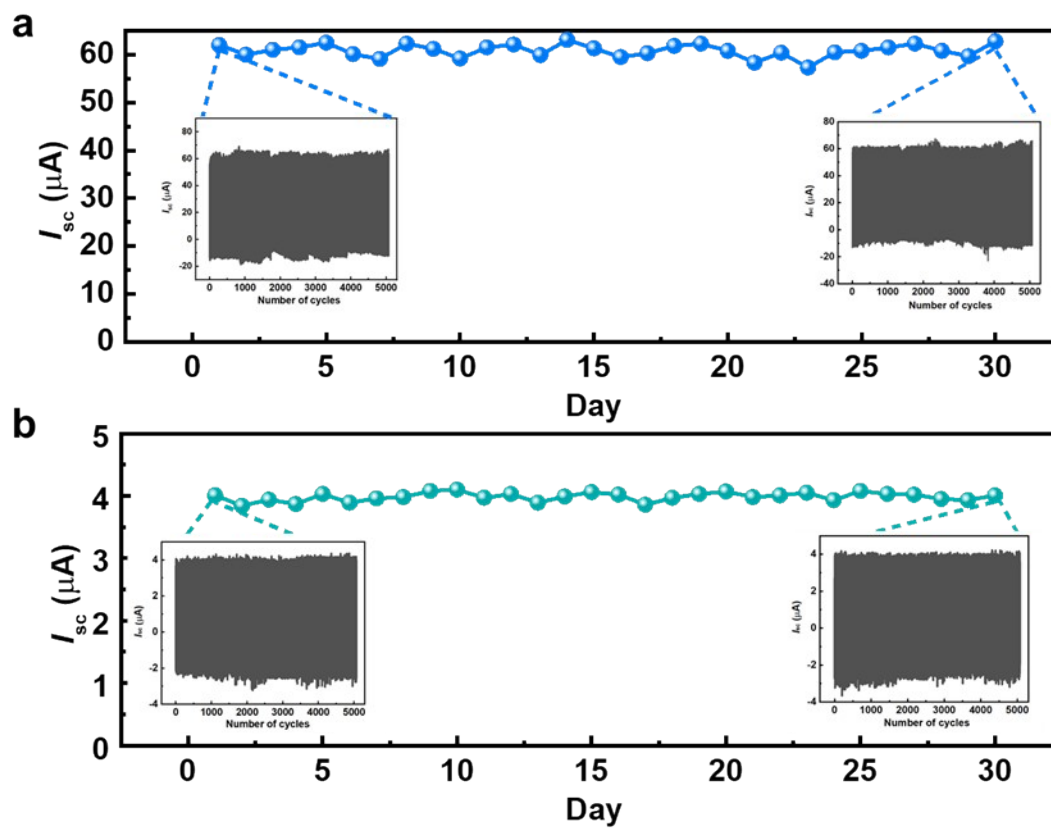


**Figure S7.** (a) Stability test of OZ module within 5200 cycles every day in one month. (b) Stability test of FL-module within 5200 cycles after one month.

We conducted the study of the effects of humidity and temperature on the OZ and FL output performances. A humidifier is applied to regulate the relative humidity in the range from 30% to 90%. It can be seen from Figure S7a, b that the  $Q_{sc}$  outputs of OZ-module and FL-module show a decreasing trend as the humidity increased, since the charges in the moisture could screen out the triboelectrification charges on the dielectric surface thus reducing the outputs. On the other hand, we repeated the humidity measurement on the well-sealed SSTE-HNG, the  $Q_{sc}$  outputs behaved relatively stable as the humidity enhanced. In addition, the impacts of temperature on the output performances of SSTE-HNG is also conducted. Due to the limited experimental conditions, we can only roughly adjust the ambient temperature within four different ranges, denotes as  $T_1$  (0-10°C),  $T_2$  (10-20°C),  $T_3$  (20-30°C) and  $T_4$  (30-40°C), respectively. The results showed that the temperature has little effect on both the OZ and FL modules as shown in Figure S7c, d.

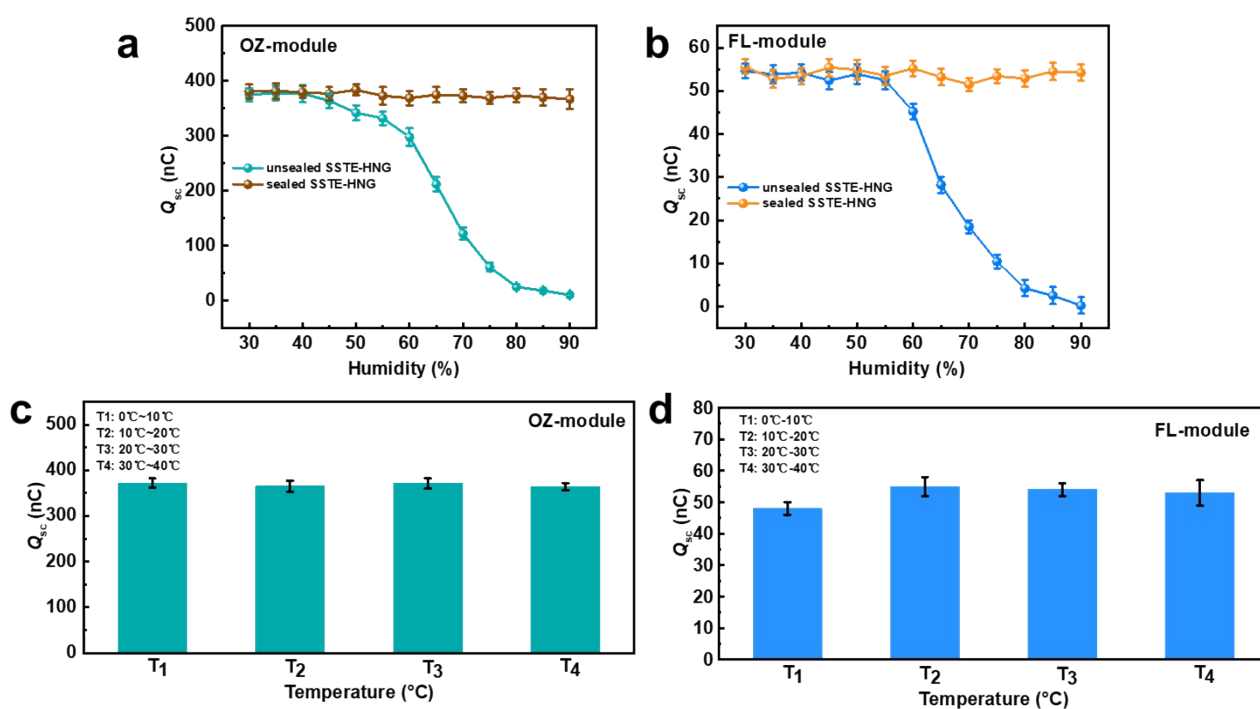


**Figure S8.** The effects of (a, b) humidity and (c, d) temperature on the OZ and FL output performances.

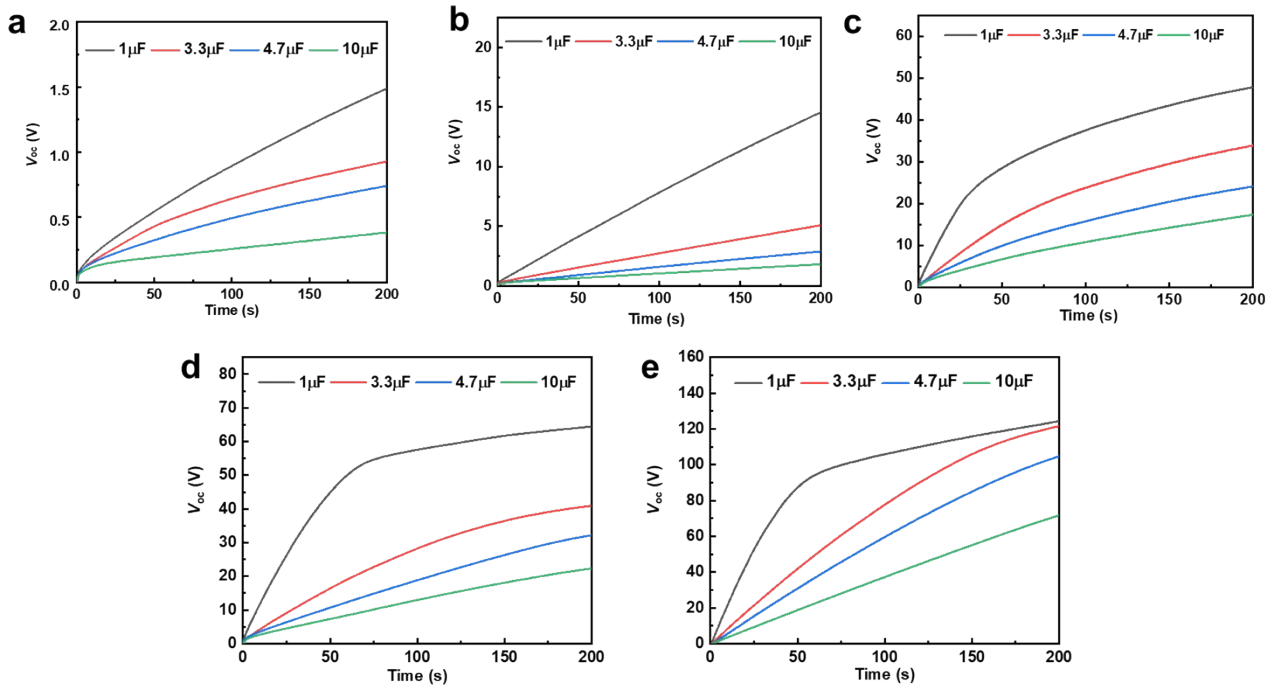


**Figure S9.** Comparisons of charging speed and voltage of individual module of (a) EMG, (b) FL and (c) OZ module. (d) Combination of FL and OZ modules. (e) Combination of FL, OZ and EMG modules for charging the capacitors ranging from  $1\mu\text{F}$ ,  $3.3\mu\text{F}$ ,  $4.7\mu\text{F}$  and  $10\mu\text{F}$  within 200s.

**Table S1.** Comparisons of power density output of peers' works using hybrid effect generators.

Structure	Year	Dielectric Material	Power Density of CS-TENG	Power Density of FR-TENG	Power Density of EMG	Reference
SSTE-HNG	2021	PDMS/PVDF/Nylon	17W/m <sup>3</sup>	4.8W/m <sup>3</sup>	9.8 W/m <sup>3</sup>	This work
R-TENG	2016	PTFE/Al		1.05W/m <sup>3</sup>	1.32 W/m <sup>3</sup>	[33]
WPHG	2016	FEP/Copper		7 mW	4.5 mW	[28]
FS-EMGs	2017	PTFE/Al	31.5 μW		66.9 μW	[27]
RF-EMG	2018	PTFE/Al	79.6 μW		90.7W	[17]
RSO-TENG	2019	PTFE/ Copper	0.5 mW		4 mW	[20]
SHNG	2019	Silicone/Copper	850 μW	165 μW	9mW	[26]
TEHNG	2019	Silicone/Nylon		67.05 mW/m <sup>2</sup>	3.8 mW/m <sup>2</sup>	[32]
PLPB-TENG	2019	PTFE/Al	22.5 mW		1.39 mW	[21]
THNG	2020	PTFE/Al		55mW/m <sup>2</sup>		[41]
SCC-TENG	2020	FEP/hair brushes		2.71W/m <sup>3</sup>	10.16W/m <sup>3</sup>	[42]
HW-NG	2021	FEP/Copper	0.41 W/m <sup>3</sup>		0.30 W/m <sup>3</sup>	[44]